2020 IEEE International Conference on Robotics and Automation (ICRA)
31 May - 31 August, 2020. Paris, France

Optimized Foothold Planning and Posture Searching for Energy-Efficient Quadruped Locomotion over Challenging Terrains

Lu Chen, Shusheng Ye, Caiming Sun*, Aidong Zhang, Ganyu Deng, and Tianjiao Liao

***Abstract*— Energy-efficient locomotion is of primary importance for legged robot to extend operation time in practical applications. This paper presents an approach to achieve energy-efficient locomotion for a quadrupedal robot walking over challenging terrains. Firstly, we optimize the nominal stance parameters based on the analysis of leg torque distribution. Secondly, we proposed the foothold planner and the center of gravity (COG) trajectory planner working together to guide the robot to place its standing legs in an energy-saving stance posture. We have validated the effectiveness of our method on a real quadrupedal robot in experiments including autonomously walking on plain ground and climbing stairs.**

I. INTRODUCTION

Legged robots have many advantages over wheeled robots when interacting with challenging uneven terrains. Once employed in a practical scenario, a quadrupedal robot is expected to work as long as possible on its task. The robot should locomote in an energy-efficient way to save energy for increasing operation time other than wasted in locomotion.

To date there have been two ways in improving the locomotion efficiency of legged robot: hardware designing (optimizing) method and algorithm designing (optimizing) approach. From the hardware point of view, some energy-efficient legged robots were developed. Based on the passive dynamics theory [1], a four-legged bipedal robot Ranger was designed which achieved a very low Total Cost Of Transport (TCOT) of 0.19 [2]. However, those passive walkers scarified the movement versatility while minimizing the power consumption. Some researchers attempted to improve legged robot locomotion efficiency by using elastic elements to temporarily store mechanical energy during locomotion. The quadruped robot ANYmal [3] and StarlETH [4] employed the series elastic actuators (SEA) to achieve high energy efficiency. The MIT Cheetah Robot [5] achieved high energy efficiency by employing a comprehensive design principle including high torque density motor design, energy regeneration and low inertia leg design. Up to now, most of existing legged robots, including quadruped robots of Boston Dynamics' BigDog, Spot and SpotMini, HyQ [6], ANYmal [3], MIT Cheetah 3 [7], Unitree's Laikago, and the biped group of the most dynamic humanoid ATLAS, ASIMO [8], and UBTECH's Walker, consume plenty of energy during operation and while untethered they can only last a few hours, or even shorter, due to their high-energy-consumption locomotion.

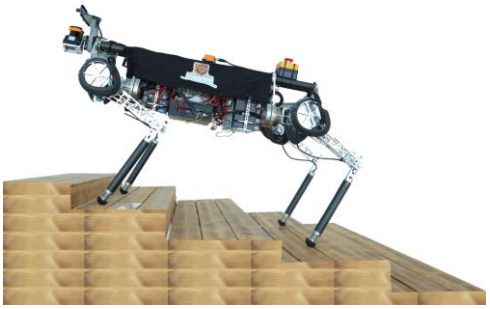

Figure 1. The quadrupedal robot Pegasus is climbing stairs.

While many creative hardware designs are achieved to increase locomotion efficiency, plenty of efforts have been paid to optimize the robot control algorithm or locomotion parameters. Hutter [9] shown an approach of changing the contact force or joint torque distribution to increase a quadrupedal robot's locomotion efficiency. An approach of generating an optimal trajectory for quadrupedal robot was presented in [10]. Compared with the distance-based search approach, the energy-based search method can generate smoother trajectory resulting less energy loss. Gait parameters are another decisive factor which influence the locomotion performance of legged robots. Many researchers have attempted to improve locomotion efficiency by optimizing gait parameters. Optimal gaits were applied on a two-legged robot to achieve walking and running in the most energetically ways [11]. The optimal gait parameters were identified by using policy gradient reinforcement learning method and realized an energy efficient dynamic walk for a NAO humanoid robot [12]. In paper [13] the foot trajectory parameters were optimized in order to achieve energy optimal locomotion for a quadrupedal robot. However, these parameter optimizing methods did not consider the terrain information resulting in low locomotion robustness when interacting with challenging terrains. Hexapod Robot Weaver can adapt its gait parameters (virtual stiffness, stride frequency, stride height) based on exteroceptive sensing and achieves a low COT on multi-terrains [14]. But leg torque workspace wasn't considered as a constraint to further reduce the energy consumption.

Our approach also makes full use of the terrain information as reported in Ref [14] and [15] while we adaptively consider leg torque distribution to achieve not only energy-efficient but also statically stable locomotion over challenging terrains. We proposed a locomotion framework which includes a foothold planner and a COG trajectory

All authors are with Institute of Robotics and Intelligent Manufacturing (IRIM), the Chinese University of Hong Kong (CUHK), Shenzhen 518172, China; also with Shenzhen Institute of Artificial Intelligence and Robotics for Society (AIRS), Shenzhen 518172, China; also with Robotics Research Center, Peng Cheng Laboratory (PCL), Shenzhen 518055, China.

*Corresponding author, Dr. Caiming SUN, cmsun@cuhk.edu.cn

optimizer working together to guide the supporting legs to form in energy-efficient stance postures.

In the following, Section II describes how we evaluated creeping static gait. Section III shows the analysis on leg torque distribution based on forward kinematics and statics. Section IV introduces the motion planner method we used for planning energy-efficient locomotion. Section V gives the results of various experiments on our quadrupedal robot Pegasus. Lastly, Section VI discusses the conclusions.

II. Static Gait Energy Consumption Analysis

A. Six Creeping Static Gait

Creeping gaits are perfect for locomotion on challenging rough terrain with low speed. They make a quadrupedal robot stay statically stable during most of a locomotion cycle [16]. Thus, we also use a six-creeping gait similar to [17] on our quadrupedal robot to achieve stable stability when walking over challenging terrains such as climbing stairs. The swing-leg sequence is right-hind (RH), right-front (RF), left-hind (LH), left-front (LF).

B. Energy Consumption Calculation

For a quadrupedal robot, equation (1) is used to calculate the total power consumption including joule heating and mechanical power during locomotion [5].

$$\begin{aligned} \text{Mechanical Power} &= \sum_{12\ motors} \tau \times \omega \\ &= \sum_{12\ motors} K_t \times I_{motor} \times \omega \\ \text{Junle Power} &= \sum_{12\ motors} I_{motor}^2 \times R \end{aligned} \quad (1)$$

where K_t is the torque constant and R is the winding resistance.

Equation (1) indicates that the joint motor current is a primary parameter in calculating the power consumption. For simpilicy, the following experiments in Section II will use the measured current to approximately indicate the power consumption.

C. Locomotion Current Analysis

To analyze how the current was consumed during locomotion, we have conducted an experiment in which the robot Pegasus walked on plain ground. Firstly, we had an analysis on the leg's three joints. Because of the same configurations of the four legs, we only take one leg (RH) for analysis. From the current profiles shown in Fig. 2a, obviously that the knee joint consumes the largest current while the hip joint consumes the least current. Secondly, the total current consumption of each leg is shown in Fig. 2b. One can observe that the leg consumes the least current when it is in swinging motion.

Therefore, the experimental results come to a conclusion that during the locomotion cycle of our quadrupedal robot Pegasus walking in six-creeping gait, the hip joint and the swinging leg consume the least current. We will design our optimization approach to minimize the current of the supporting legs including thigh joint and knee joint while neglect the swinging leg.

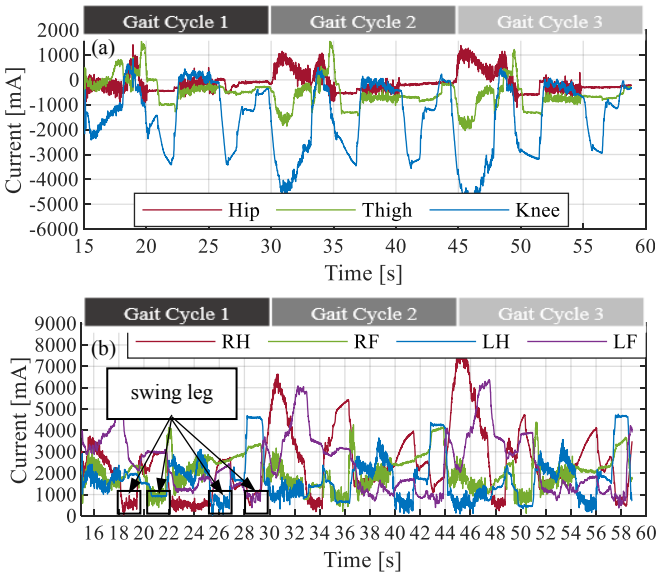

Figure 2. (a) RH leg joint current during a three full gait cycles locomotion. The knee joint current (avg 1611 mA, max 5140 mA) is much larger than the hip (avg 351 mA, max 1628 mA) joint. At most of the time, the hip joint current is near zero thus can be neglected. (b) The current consumption of the four legs in a three gait cycles locomotion. The swinging leg has the least current whose value is below 1000 mA (shown as the four solid black rectangles).

III. Leg Workspace And Torque Distribution

To find out the energy-saving workspace for a leg, we need to get the leg torque distribution in two steps. Firstly, we derived the leg workspace in x and z coordinate plane that the hip joint is neglected. Then we calculated the torque values of thigh and knee joints through the entire leg workspace based on statics analysis.

A. Leg Workspace

Figure 3 shows the kinematics configurations of our quadrupedal robot Pegasus. The robot body coordinate frame is defined at the same point of COG which is at the same height of hip joint. Here we neglect the link length between hip joint and thigh joint whose length is 0.08 m. Therefore, the coordinate origins of those two joints (P_{HIP}, P_0) are assumed to be at the same coordinate point. For convenience the cartesian positions of knee joint and foot joint calculated from forward kinematics are in the hip coordinate frame.

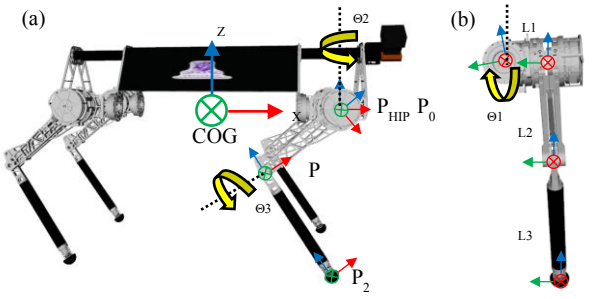

Figure 3. Leg joints configuration and frame definition of the quadrupedal robot Pegasus. The 3DOF leg joints are configured as hip (roll), thigh (pich) and knee (pitch). (a) Side view. (b) Back view.

The forward kinematics equations are shown as (2), where for Pegasus, L_2 is 0.26 m, L_3 is 0.34 m.

$$\begin{aligned} x_0 &= x_{hip} \\ y_0 &= y_{hip} - L_1 \cos\theta_1 \\ z_0 &= z_{hip} + L_1 \sin\theta_1 \\ x_1 &= x_0 + L_2 \sin\theta_2 \\ y_1 &= y_0 - L_2 \sin\theta_1 \cos\theta_2 \\ z_1 &= z_0 - L_2 \cos\theta_1 \cos\theta_2 \\ x_2 &= x_1 + L_3 \sin(\theta_2 + \theta_3) \\ y_2 &= y_0 - \sin\theta_1 \left[L_2 \cos\theta_2 + L_3 \cos(\theta_2 + \theta_3)\right] \\ z_2 &= z_0 - \cos\theta_1 \left[L_2 \cos\theta_2 + L_3 \cos(\theta_2 + \theta_3)\right] \end{aligned} \quad (2)$$

B. *Torque Distribution*

Pegasus weights about 35.2 kg, each leg shares approximately 86.2 N force when standing in nominal stance. For a nominal stance, we take an analysis of the statics on each leg. The inferred statics expressions of our Pegasus robot are shown in (3).

$$\begin{aligned} T_{thigh} &= -[L_2 \sin\theta_2 + L_3 \sin(\theta_2 + \theta_3)] f_x \\ &\quad + [L_2 \cos\theta_2 + L_3 \cos(\theta_2 + \theta_3)] f_z \\ T_{knee} &= -L_3 \sin(\theta_2 + \theta_3)\, f_x + L_3 \cos(\theta_2 + \theta_3)\, f_z \end{aligned} \quad (3)$$

Based on the forward kinematics equation (2) and statics equation (3), the leg torque distribution can be drawn as shown in Fig. 4. The torque distribution is used for finding out the torque-saving leg stance posture. Because we focus on optimizing the torque distribution for supporting legs, the force implied on foot in horizontal direction is neglected, i.e., $f_x = 0$. Obviously, the torque on thigh joint and knee joint is proportional to the weight distributed from the trunk. Though the torque distribution discussed in this section is generated based on the assumption that the four legs bear the same weight, the leg torque has the same distribution (only the torque value is different) no matter where the placements of the four legs are. Thus, the torque distribution shown in Fig. 4 is general enough for analyzing energy consumption of the supporting legs during locomotion.

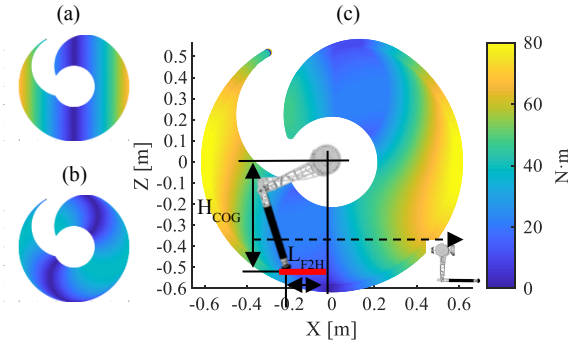

Figure 4. Torque distribution of leg. Darker blue stands for smaller torque values. (a) Thigh joint torque distribution. The thigh joint has the minimum torque value when the foot placement is just below the center of thigh joint, demonstrated as the darkest blue zone. (b) Knee joint torque distribution. The knee joint has the minimum torque value if the foot stands behind some distance to the thigh joint. (c) Sum of thigh and knee joint torque distribution. The total minimum torque value only appears if the leg stands up straightly. The zone (we will specifiy an torque-saving workspace in this zone) bewteen the thigh joint and knee joint's minimum torque line have smaller torque values compared to other zone'.

When searching for the torque-saving workspace, the kinematics constraint and static stability constraint must be considered together. Though some workspace has the minimum torque but not meet the kinematics constraint or stability constraint, this workspace should be avoided. Firstly, the COG height (HCOG) should be larger than the thigh link length (L2) to avoid the knee joint from touching the ground (shown as the dashed line in Fig. 4c). Secondly, the leg should not stand straightly to avoid influencing the locomotion stability.

To help find out the torque-saving workspace, we have validated the leg torque distribution by commanding our quadrupedal robot to move up and down alternately. The experiment results shown in Fig. 5 demonstrate that the current on leg joints have the extreme values in some specific postures. One can observe that the minimum current (torque) value occurs when the leg is almost completely bended (Fig. 5a) or nearly stretched straightly (Fig. 5c). And the maximum value appears when the leg is at about the center position (Fig. 5b) in an up-down cycle. This conclusion is approximately the same as the leg torque distribution.

The torque-saving workspace is parameterized by two parameters H_{COG} (the height from foot to hip joint) and L_{F2H} (the horizon distance from foot to hip joint). According to the analysis on torque distribution and experiment results, we get a suggested torque-saving workspace (the red filled rectangle shown in Fig. 4c) for our quadrupedal robot Pegasus. The settings for the two parameters H_{COG} and L_{F2H} is [0.48 m, 0.52 m] and [0, -0.2 m] (minus sign demonstrates that foot joint is behind hip joint).

IV. Energy-Efficient Based Motion Planner

A. *Optimized Nominal Stance*

For the six-creeping gait, in each gait cycle there are two nominal stances appearing alternately. The shape of nominal stance plays an important role in locomotion stability and moving speed [18]. A nominal stance with shape of parallelogram is widely used in statically walking gait of quadrupedal robot.

In this paper we parameterize our robot's nominal stance with three parameters: stance length (LStance), stance width (WStance) and skew (LSkew), depicted in Fig. 6a. The skew is a key parameter which helps the robot to move faster and more stable [18]. We experimentally found that robot walks more stable and faster if the skew is equal to half of step length.

The following will discuss the gait parameter constraints. We assume the robot is moving forward only and the static stability can be fit at all time. First, the leg must be avoided stretching straightly at any time. There exist two situations in which the leg is easy to stretch straightly. The first one is the hind leg (Fig. 6b) in the body shifting stage when climbing

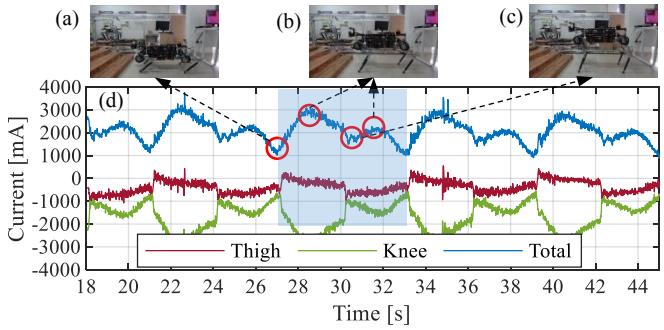

Figure 5. The up-down experiment. The robot stands in a predefined stance location where the four feet are below the thigh joint. This figure shows the current changing trend of the RH leg including the hip joint, thigh joint and knee joint during up-down movement.

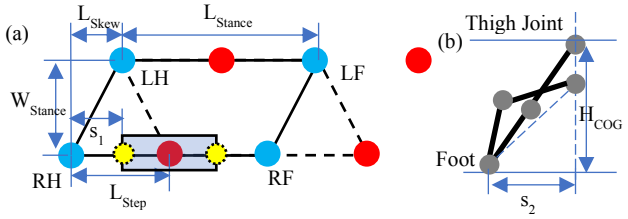

Figure 6. (a) The nominal stance. Solid line parallelogram is the nominal stance when right two legs are swinging, dashed line parallelogram is the nominal stance during left two legs swing stage. The narrow rectangle is the foothold search region with nominal foothold at center and min and max foothold (yellow sphere) at two sides. (b) To avoid a leg from stretching, the square sum of s_2 and H_{COG} must be less than the square of leg length.

stairs. This kinematical constraint of leg can be described as equation (6). The second one is in the leg swinging stage, the swinging leg may extend to its limit with a very large step length. This kinematical limitation can be expressed in equation (7). Furthermore, it should be noted that when the foothold is planned at the left edge (shown as the dashed yellow sphere in Fig. 6a) of search rectangle. After each swing-leg stage, the flying foot should be ahead of its previous location once touched ground ($s_1 > 0$). This constraint is shown as equation (5). Lastly, shown as equation (4), we set the skew value to half of nominal step length to achieve a stable locomotion stability.

The following summarized gait constraints are used to guide our robot locomotion parameters settings.

$$L_{\text{Skew}} = L_{Step}/2 \tag{4}$$

$$L_{\text{Search}} < 2L_{Step} \tag{5}$$

$$L_{Step} < \sqrt{L_{Leg}^2 - H_{COG}^2} \tag{6}$$

$$L_{\text{Search}} < 2\sqrt{L_{Leg}^2 - H_{COG}^2} - L_{Step}/2 \tag{7}$$

For Pegasus, the leg length L_{Leg} is 0.6 m. To achieve high energy-efficient locomotion, leg torque distribution is considered as a critical constraint (in Fig. 6) to obtain gait parameter settings as followed: COG height H_{COG} is close to 0.5 m in the recommended energy-saving workspace. According to constraint (6), we can calculate the step length should be set less than 0.33 m. Here we set L_{Step} to 0.2 m. Based on constraint (5) and (7), the length of foothold search rectangle should be less than 0.4 m. We set L_{Search} to 0.3 m. A small value 0.08 m is set as the width of search rectangle accounting for the lateral locomotion limitation.

B. Foothold Planner

For a quadrupedal robot, the foothold planner plays a key role in ensuring safe locomotion on challenging terrains. Given the optimized nominal stance as the starting position (in Fig. 7a), the foothold planner can select a list of kinematical feasible foothold locations to the goal position. In addition, the selected candidate footholds must can be formed in the optimized nominal stance when the energy-efficiency constraint is considered. The leg torque distribution actively contributes to our foothold planner together with kinematic analysis on terrain maps, which leading to energy-efficient postures for legged robots on challenging terrains. Our proposed foothold planner has a cascaded structure that applies different length of rectangular search region until valid footholds are found (Fig. 7). The main components of the planner are described in the following sections.

1) Traversability Map:

The traversability map is created from the elevation map. Similar to [19], the traversability score can be generated from the geometrical characteristics of the terrains including height of step, angle of slope and roughness of terrain. The higher of the score is, the higher of the locomotion traversability is.

2) Foothold Feasible Score:

Based on the traversability map and taking the toque

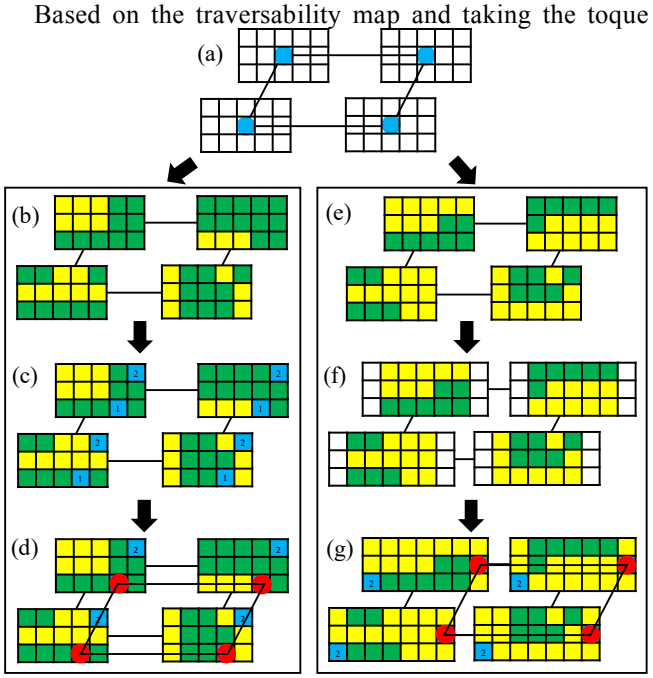

Figure 7. The foothold planner is searching for footholds which can form in optimized nominal stance. (a) The initial stance. As a demonstration, the search region includes 9 cells (3×5) with nominal foothold in the center shown as the blue sphere. (b) The traversability score map of search region with green cells stand for valid while yellow cells are invalid. (c) Searching for the cells (blue cells with the number stands for its prioity) which can form nominal stance. (d) The final footholds are found shown as the red spheres forming in a nominal stance. (e) Another case of traversability score map. (f) Because of no valid cells are found that can form in nominal stance, the search rectangle length is broaden (3×7). (g) The final footholds are found.

distribution into account, the foothold feasibility f ∈ [0,1] combines the values as below:

$$f = 1 - \omega_1 \frac{d_1}{D_1} - \omega_2 \frac{d_2}{D_2} \tag{8}$$

$$\begin{cases} \omega_1 + \omega_2 = 1 \\ D_1 = \frac{L_{Search} + W_{Search}}{2} \\ D_2 = \frac{W_{Search}}{2} \end{cases} \tag{9}$$

where d_1 is the Manhattan Distance from the nominal foothold to the planned foothold while d_2 is the Euclidean Distance to center line of the two long edges of search rectangle. The weights ω_1 and ω_2 can penalize footholds whose distance to the nominal foothold location is far away from forward and lateral direction respectively.

3) Foothold Searching Procedure:

Similar to the quadrupedal robot ANYmal [20], our foothold planner starts the searching progress from the nominal foothold in a specific search region of a nominal stance (shown as Fig. 7a). The searching strategy is improved that the leg torque workspace is incorporated as a critical constraint for the optimization of energetically efficient locomotion. Additionally, a narrow rectangle is used instead of a circle as the search region since the workspace of forward motion is of more importance than the workspace of the lateral motion when the quadrupedal robot is in forward locomotion. Furthermore, our foothold planner supports any specified number of foothold locations, for example 4, 8, or 12 footholds, etc. in one planning cycle.

The foothold planner searching progress for the next gait cycle is as below: By using the traversability score map (shown as Fig. 7b), the planner finds all the kinematical valid footholds (also called candidate footholds, shown in Fig. 7c) which can form in nominal stance. Then the feasibility score values of the candidate footholds are computed according to equation (8) and (9). Lastly, the candidate footholds with the highest priority in each search region is chosen as the final footholds for the next gait cycle (Fig. 7d). Should this cascade not result in feasible footholds (Fig. 7e), the search rectangular regions are extended by a pre-specified length (Fig. 7f) and the cascaded searching process is repeated. If no valid footholds are found after the second run through the cascade, the foothold which is closest to the nominal foothold is chosen as the final foothold.

C. COG Trajectory Planner

We have also proposed a COG trajectory generator which can adapt itself to terrain. Each gait cycle includes two main points (also called waypoints) which determine the COG trajectory when robot is in stance with four feet after the trunk-shifting stage. The feet locations which form the supporting triangle are used to calculate the triangle inner center (the COG waypoint). As the footholds are planned based on the percept terrain elevation map, the COG waypoints will adapt the terrain accordingly. The height of COG is defined as the mean height of supporting feet. Lastly, we set a threshold to suppress the trunk fluctuation. If the variations of COG height did not exceed the fluctuation threshold, the height of the COG remains unchanged.

D. Navigation Framework

Given a navigation goal, the robot should be able to reach that goal as efficiently as possible. To achieve this self-navigation ability, several functional modules such as localization, perception and mapping, foothold planning, swing-leg trajectory planning and COG trajectory planning are needed to be organized together appropriately. The locomotion planning frameworks we proposed is shown in Fig. 8. It should be noted that the modules marked with red rectangle are the key components in this paper to realize the robot automatically walk in energy-efficient locomotion over challenging terrains. The foothold planner together with the COG trajectory planner guide the robot to walk in a way that using the optimized nominal stance which is created based on the leg torque distribution.

The robot uses a rotating 2D lidar to perceive the surrounding terrain information. The scanned data are reconstructed as 3D point cloud which are used for generating the elevation map. An open source elevation mapping Robot Operating System (ROS) package [21] is used in our project. The traversability map is created based on the elevation map. Once the feasible footholds are found based on the traversability map, the COG trajectory and the collision free swing-leg trajectory can be planned. The footholds together with the trajectories in cartesian space are transformed into leg motor's position in joint space which are used to control the legs to form in energy-saving stance posture.

To correct the accumulation errors caused by slipping, we designed an auxiliary localization module based on 3D point cloud. This module follows the center of a randomly selected object in front of robot. The changed coordinate transformation between robot and object is used to correct the localization errors in odometer module.

V. EVALUATIONS

We have validated the approach on our quadrupedal robot.

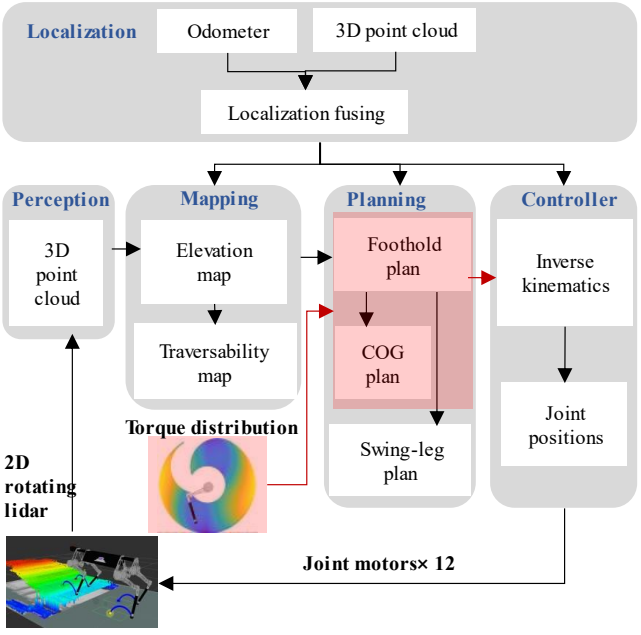

Figure 8. An overview of Pegasus navigation framework.

Pegasus is about 1.0 m long, 0.4 m wide, and 0.75 m tall when legs stand straightly, with weight of about 35.2 kg. The 3DOF legs are driven by electric motors at 400 Hz by PD position controller. A NVIDIA Jetson TX2 embedded computer is used as the center computing platform. A Hokuyo UTM-30LX-EW lidar is mounted on the robot head to perceive the surrounding map. The lidar can sweep a full scanning at about 1.5 s. The optimization parameters for energy-efficient locomotion used in our experiments are summarized in Section IV.

A. *Walking on Plain Ground*

The first experiment was walking on plain ground. The quadrupedal robot walks twice at the same distance but with two different planning parameters. The first setting use the traditional parameters while the other uses optimized parameters. We use equation (1) to calculate the total power consumption in locomotion experiments. For Pegasus, the torque constant $K_t = 0.217$ Nm/A, the winding resistance $R = 2.28\ \Omega$. Fig. 10a shows the locomotion power consumption.

B. *Climbing Stairs*

The second experiment is climbing a set of stairs shown as Fig. 1. The stairs have a rise of 8 cm and a run of 30 cm. To make sure that the robot travels approximately the same distance during the two comparative experiments, the robot is set to start from the same origin position and halt until the last foot successfully climbs the last step.

With optimized gait parameters, our motion planner can help the robot to keep its legs standing in energy-saving postures during climbing stairs. As a result, the optimized locomotion achieved a lower power consumption. It is interesting to note the duration (15~50 s in Fig. 10b) when the robot is in a nominal stance with all four feet touched ground (Fig. 9a) waiting for mapping. In this duration, the power consumption in an optimized nominal stance (green line) is much less than that of in non-optimized stance (red line).

Table I details the power consumed during auto locomotion on plain terrain and climbing stairs. We can see that by using our proposed motion planner with optimized gait parameters results in an energy consumption reduction of 13.6 % for plain ground and 7.94 % for stairs compared to non-optimized gait. Additionally, our robot COT during the two experiments can be given by the power consumption

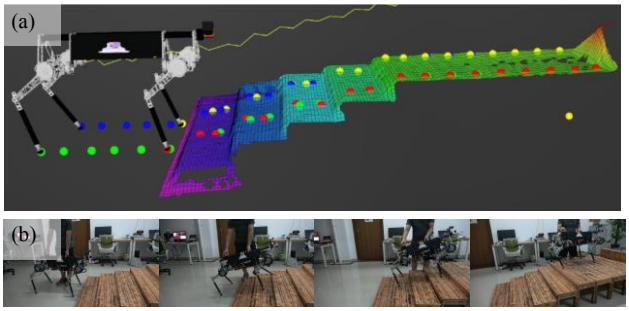

Figure 9. The robot is climing stairs. (a) Before locomotion, the robot plans a global COG trajectory (yellow line) along with a list of global footholds (color spheres, red-RF,green-RH, blue-LH, yellow-LF) on the percept terrain elevation map. (b) Sequence of snapshots of Pegasus while climing the stairs.

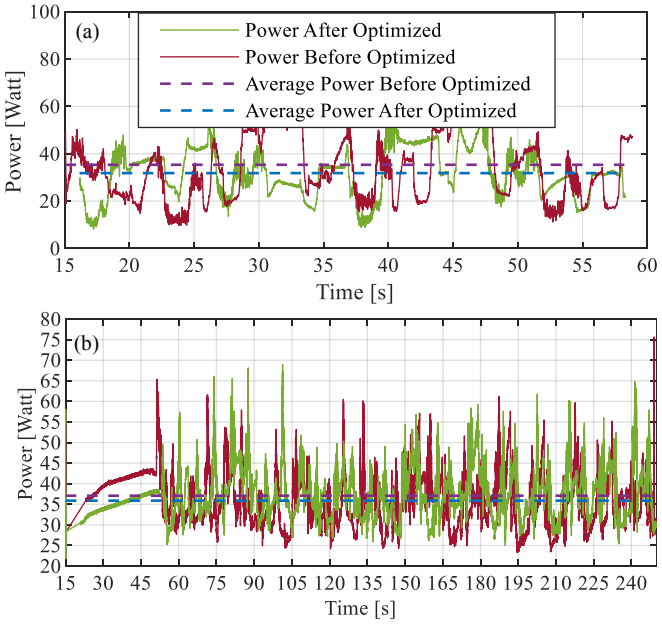

Figure 10. Power consumption. (a) Walkinig on plain terrain in three full gait cycles. (b) Climing stairs.

TABLE I. PEGASUS POWER CONSUMPTION DURING WALKING ON PLAIN GROUND AND CLIMBING STAIRS

	Avg Before Optimized	Total Before Optimized	Avg After Optimized	Total After Optimized
Ground	35.4 w	150210 w	31.8 w	132170 w
Stairs	37.8 w	851110 w	35.2 w	783490 w

divided by the weight times velocity [2]. Compared to other legged robots such as Boston Dynamics BigDog (COT=15) [5], Hexapod Robot Weaver (COT=36.43) [14], our robot COT is 7.68 for plain ground and 8.2 for stairs, demonstrating the effectiveness of our proposed approach in improving locomotion efficiency. Moreover, other legged robots, such as BigDog or Weaver can also use this approach to reduce their COT by about 10% or more.

VI. CONCLUSION

The experimental results demonstrate that by controlling the robot postures to make legs stay in energy-saving workspace with the help of foothold planner and COG planner, the quadrupedal robot can achieve a more energy-efficient locomotion both on plain ground and rough terrain. Our Pegasus robot can continuously walk on challenging terrains for over 24 hours with one cycle of battery operation time.

ACKNOWLEDGMENT

This work was supported in part by the National Natural Science Foundation of China (Grant No. U1613223), in part by the Shenzhen Natural Science Foundation (Grant No. JCYJ20180508163015880), and in part by funding from Shenzhen Institute of Artificial Intelligence and Robotics for Society (AIRS), Shenzhen 518172, China, and Peng Cheng Laboratory (PCL), Shenzhen 518055, China.

REFERENCES

[1] McGeer T. Passive dynamic walking[J]. I. J. Robotic Res., 1990, 9(2): 62-82.

[2] Bhounsule P A, Cortell J, Ruina A. Design and control of Ranger: an energy-efficient, dynamic walking robot[M]//Adaptive Mobile Robotics. 2012: 441-448.

[3] Hutter M, Gehring C, Jud D, et al. Anymal-a highly mobile and dynamic quadrupedal robot[C]//2016 IEEE/RSJ International Conference on Intelligent Robots and Systems (IROS). IEEE, 2016: 38-44.

[4] Hutter M, Remy C D, Hoepflinger M A, et al. Efficient and versatile locomotion with highly compliant legs[J]. IEEE/ASME Transactions on Mechatronics, 2012, 18(2): 449-458.

[5] S. Seok, A. Wang, Chuah, M. Y. (Michael), D. Otten, J. Lang, and S. Kim, "Design principles for highly efficient quadrupeds and implementation on the mit cheetah robot," in 2013 IEEE International Conference on Robotics and Automation, 2013.

[6] Semini, C, et al. "Design of HyQ – a hydraulically and electrically actuated quadruped robot," Proceedings of the Institution of Mechanical Engineers, Part I: Journal of Systems and Control Engineering, 225(6), 831–849, 2011.

[7] Bledt G, Powell MJ, Katz B, Carlo J, Wensing P, Kim S, "MIT Cheetah 3: Design and Control of a Robust, Dynamic Quadruped Robot." IEEE/RSJ International Conference on Intelligent Robots and Systems (IROS), 2018: 2245 - 2252.

[8] Sakagami, Y., Watanabe, R., Aoyama, C., Matsunaga, S., Higaki, N. and Fujimura, K. "The intelligent ASIMO: system overview and integration, " In Proc. of IROS, 2002, 2478- 2483.

[9] Hutter M, Gehring C, Bloesch M, et al. Excitation and stabilization of passive dynamics in locomotion using hierarchical operational space control[C]//2014 IEEE International Conference on Robotics and Automation (ICRA). IEEE, 2014: 2977-2982.

[10] Harper M Y, Nicholson J V, Collins E G, et al. Energy Efficient Navigation for Running Legged Robots[C]//2019 International Conference on Robotics and Automation (ICRA). IEEE, 2019: 6770-6776.

[11] Xi W, Remy C D. Optimal gaits and motions for legged robots[C]//2014 IEEE/RSJ International Conference on Intelligent Robots and Systems. IEEE, 2014: 3259-3265.

[12] Sun Z, Roos N. An energy efficient dynamic gait for a nao robot[C]//2014 IEEE International Conference on Autonomous Robot Systems and Competitions (ICARSC). IEEE, 2014: 267-272.

[13] Koco E. Locomotion Control for Electrically Powered Quadruped Robot Dynarobin[C]//Advances in Cooperative Robotics, Proceedings of the 19th International Conference on CLAWAR 2016. 63-70.

[14] Bjelonic M, Kottege N, Homberger T, et al. Weaver: Hexapod robot for autonomous navigation on unstructured terrain[J]. Journal of Field Robotics, 2018, 35(7): 1063-1079.

[15] Chen, L., Ye, S., Sun, C., Zhang, A., Deng, G., Liao, T., & Sun, J. (2019, December). CNNs based Foothold Selection for Energy-Efficient Quadruped Locomotion over Rough Terrains. In 2019 IEEE International Conference on Robotics and Biomimetics (ROBIO) (pp. 1115-1120). IEEE.

[16] R. B. McGhee, A. A. Fkask, and A. Frank. On the stability properties of quadruped creeping gaits. Mathematical Biosciences, 3:331–351, Aug. 1968.

[17] Hutter M, Sommer H, Gehring C, et al. Quadrupedal locomotion using hierarchical operational space control[J]. The International Journal of Robotics Research, 2014, 33(8): 1047-1062.

[18] Pongas D, Mistry M, Schaal S. A robust quadruped walking gait for traversing rough terrain[C]//Proceedings 2007 IEEE International Conference on Robotics and Automation. IEEE, 2007: 1474-1479.

[19] Wermelinger M, Fankhauser P, Diethelm R, et al. Navigation planning for legged robots in challenging terrain[C]//2016 IEEE/RSJ International Conference on Intelligent Robots and Systems (IROS). IEEE, 2016: 1184-1189.

[20] Fankhauser P, Bjelonic M, Bellicoso C D, et al. Robust rough-terrain locomotion with a quadrupedal robot[C]//2018 IEEE International Conference on Robotics and Automation (ICRA). IEEE, 2018: 5761–5768.

[21] Fankhauser P, Bloesch M, Gehring C, et al. Robot-centric elevation mapping with uncertainty estimates[M]//Mobile Service Robotics. 2014: 433-440.